Constraints on Slow Earthquake Dynamics from a Swarm in Central Italy

Luca Crescentini,[1,2]* Antonella Amoruso,[2,3] Roberto Scarpa[2,3]

Several clustered slow earthquakes have been recorded by a geodetic interferometer in central Italy. The strain rise times of the events range from tens to thousands of seconds, and the seismic moment scales with the square root of the rise time. This scaling law contrasts with the conservative assumption of constant rupture velocity in fault modeling but is consistent with the occurrence of a slow rupture propagation analogous to heat diffusion in a slab.

Slow earthquakes have been observed in Japan and California as nearly exponential strain changes with durations ranging from about 1 hour to 3 days and strain steps larger than 3×10^{-8} (*1–4*). Indirect evidence for slow earthquakes comes from seismograms with anomalous long-period spectral behavior (*5–9*). In these cases, the durations of the slow earthquakes range from a few seconds (*5*) to a few hundred seconds (*6–9*), but there is no general acceptance among the geophysical community of the need to invoke slow earthquakes to explain low-frequency amplitude and phase anomalies (*10*). Slow earthquakes not only suggest that faults can sustain ruptures over a wide range of time scales but also that the slowness can be in the rupture velocity (slow rupture propagation) (*3*), in a low slip rate (a long rise time, that is, a long time for slip to achieve 63% of its peak value) (*4*), or both. No scaling relation between seismic moment and duration has been determined.

A geodetic interferometer is located 1400 m under the free surface in a seismically active region of the Apennines, central Italy, beneath Gran Sasso (42°28′N, 13°34′E) (*11*). We analyzed 180 slow strain changes, mainly gathered during one sequence that started on 21 March 1997 (Figs. 1 and 2) (*12*). The large number of slow signals are for small-amplitude strain changes (4×10^{-10} to 2×10^{-8}) and the lack of similar observations reported in the literature could be due to lower sampling rates (*2, 4*), higher noise levels, irregular worldwide distribution of slow earthquakes (*7*), or lack of appropriate instrument sensitivity to detect signals like those we report.

From March 1997, a few seismic swarms occurred within a radius of 200 km from the interferometer (Figs. 2 and 3), after more than 1 year of background diffuse seismicity during which only two minor swarms took place. The swarms were characterized by magnitudes up to 4.1 and were concentrated into three main sequences named Matese, Massa Martana, and Colfiorito. The Colfiorito sequence was the beginning of the Umbria-Marche 1997–98 sequence.

It is unlikely that the three seismic sequences had any direct effect on producing the strain changes seen at Gran Sasso because of the small amplitude of the seismic waves and of the coseismic deformations. Occurrence times of the slow events are random relative to the times of the seismic transit beneath the instrument. No correlation has been found with meteorologic data (temperature, air pressure, or rainfall), regional earthquakes, worldwide large earthquakes, or events detected by the local short-period seismic network, managed by Servizio Sismico Nazionale (threshold $M_l \sim 1$). The interferometer has never recorded similar signals during the transit of either long-period surface waves from distant earthquakes or short-period body waves from local earthquakes. The slow events were not more frequent by day than by night or at any one particular hour, and no unusual activity occurred in the nearby underground nuclear physics laboratories during their occurrence period.

After removing the effects of the tides from the strain data (*13*), we fitted an exponential function to each slow event to retrieve the amplitude and rise time of the strain change (Fig. 4). Independently of the occurrence time, the location of the contemporaneous seismic swarm (Fig. 2), or the sign of the signals (26 of the 180 events give a negative difference between the extension of the baseline perpendicular to the Apennines and the extension of the baseline parallel to the Apennines), nearly all of the points are distributed between a straight line parallel to the best-fit one (slope = 0.5), and the threshold level.

A slipping fault generates a displacement field at a distance R mainly composed of an elastic wave train $u_w(R,t)$ and of a quasi-static component $u_s(R,t)$. Both quantities are actually vectors and depend on the azimuth of the observer, but $u_w(R,t) \approx \dot{M}_0(t - R/\beta)/(\mu\beta R)$ (far-field component) and $u_s(R,t) \approx M_0(t - R/\beta)/(\mu R^2)$ (intermediate-field component), where $M_0(t - R/\beta)$ is the delayed time-dependent seismic moment, $\dot{M}_0(t - R/\beta)$ is the delayed moment rate, μ is the rigidity, and β is the wave speed, here assumed to be independent of frequency (*14*). Strain, ϵ, can be obtained by differentiating displacement with respect to R, thus $(\epsilon_w/\epsilon_s) \approx (R/\beta\tau)$, where τ is the characteristic time of the seismic moment time function. In our observations, the strain step is much larger than the radiated pulse, so that signals relate to the intermediate-field component and strain scales with $1/R^3$. If sources were distributed at random distances from the interferometer, points in Fig. 4 would be scattered. Thus, spatially clustered sources are more likely. Their distance from the instrument is $\lesssim$100 km; otherwise, the far-field component of the shortest events ($\tau \approx 10$ s) would have been recorded. The area in the Matese region, which was seismically active when the slow event rate took its major excursion, is about 140 km from the interferometer, too far to be the source region for the slow events.

If the seismic moment of the largest slow events is similar to that of the strongest earthquakes of the ordinary swarms, and the sources of the slow events share the same geometric characteristics of ordinary seismic sources in the Apennines (*15*), a possible source lo-

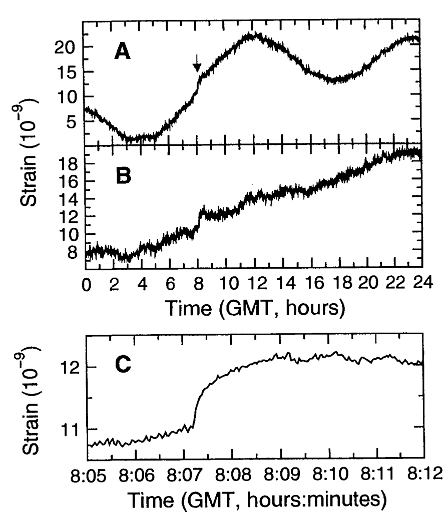

Fig. 1. Slow earthquake recorded by the Gran Sasso underground geodetic interferometer on 15 February 1997. The two upper plots show a whole day of data resampled every 20 s, (**A**) before and (**B**) after removing tides. The slow earthquake is indicated by the arrow. (**C**) is a magnified view of the slow event, sampled every 2 s. Amplitude and rise time are about 10^{-9} and 26 s, respectively. GMT, Greenwich mean time.

[1]Dipartimento di Scienze della Terra, Università di Camerino, Camerino (MC), Italy. [2]Istituto Nazionale di Fision Nucleare–Laboratori Nazionali del Gran Sasso (LNGS), L'Aquila, Italy. [3]Dipartimento di Fisica, Università di L'Aquila, L'Aquila, Italy.

*To whom correspondence should be addressed. E-mail: crescentini@camserv.unicam.it

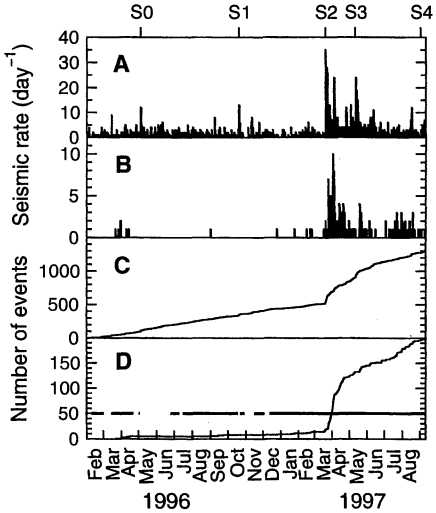

Fig. 2. Seismicity and slow events from 1 February 1996 to 9 September 1997. Both the rates (in events per day) and the cumulative number of events are shown. (**A**) and (**C**) refer to earthquakes in a radius of 200 km from the interferometer (data kindly provided by Istituto Nazionale di Geofisica). Starting times of the seismic swarms (S0, Barrea; S1, Gabbia; S2, Matese; S3, Massa Martana; S4, Colfiorito) (Fig. 3) are indicated; the other peaks in (A) arise from fluctuations in background diffused seismicity or to secondary maxima of the sequences (the highest peak between S2 and S3 is due to the second part of the Matese sequence, which came to an end before S3 started). (**B**) and (**D**) refer to the slow events recorded by the interferometer. The rate of slow earthquakes presents a secondary maximum contemporaneous to S3. Slow activity continued between S3 and S4, which started at the end of the working period of our interferometer and included thousands of seismic events. Running time of the interferometer is given by the thick horizontal line in (D); note that it was not working during the minor swarms S0 and S1.

cation might be 20 km south of the interferometer, in a well-known seismic area that was not observed to be active from 1 February 1996 to 9 September 1997. Modeling of a typical Apennine fault (*15, 16*) shows that rotating the slipping fault by a few degrees can lower the signal amplitude or even change its sign. For each rise time, the largest signals would originate from the best oriented faults (with respect to observation of a deformation signal), while the worst oriented faults would give smaller signals.

Causal interconnections of seismicity patterns in Italy and in adjacent regions and possible propagations of strain pulses along the Apennines have been suggested in the past (*17*) from seismic catalog analysis. If the proposed picture is correct, it gives direct evidence of contemporaneous swarms of slow earthquakes and low-magnitude ordinary earthquakes in different places (Figs. 2 and 3). Although triggered seismicity, even at long distances from the triggering event, has been observed after the 1992 Landers, California, USA, earthquake (*18*), the explanation in that case involved large dynamic strains accompanying seismic waves. In our case, space-time distributions of the slow earthquakes and of the ordinary seismic swarms and the lack of any cause-and-effect relation suggest that they may be the consequence of a single stress redistribution phenomenon affecting a large area of the Apennines.

Because the intermediate field strain is proportional to the time-dependent seismic moment $M_0(t)$, the observed relation between amplitude A and rise time τ ($A \propto \sqrt{\tau}$) implies the same scaling law between seismic moment and rise time ($M_0 \propto \sqrt{\tau}$). The relation of seismic moment to rise time is different from that expected in the case of earthquakes (*19*). If confirmed, this scaling relation puts constraints on slow earthquake dynamics and more generally on fault mechanics. Although a slow slip rate might be predicted by rate-state friction laws (*20*), no theoretical scaling relation has been developed. Amplitudes and rise times of prior observations related to slow slipping (*2, 4*) do not seem to follow any scaling law. The Sanriku-Oki (*3*) and the Izu-Oshima (*21*) slow earthquakes were modeled and ascribed to slow rupture propagation. Their seismic moments (1×10^{20} to 4×10^{20} N·m and about 5×10^{19} N·m, respectively) were much larger than expected from Fig. 4, probably because of the completely different tectonic setting in Japan compared to Italy, but approximately scale with the square root of their durations (1 day and 1 hour). The main slow earthquake (unmodeled, but maybe related to slow rupture propagation, like the other Japanese events) and the associated foreshocks and aftershocks in the Irako borehole strainmeter record of 25 August 1976 (*21*) also scale with the square root of their durations.

To explain the observed scaling law, we considered a one-dimensional (1D) array of slider blocks connected by springs. Slipping is resisted by a dynamic friction proportional to the slip rate (a simple type of velocity-strengthening friction). Slip propagation between adjacent blocks is the equivalent of the rupture

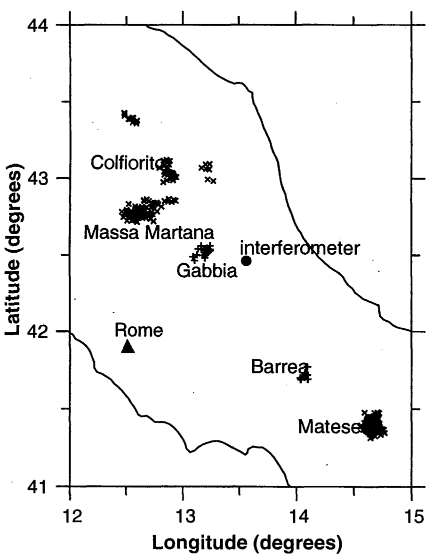

Fig. 3. Location of the laser interferometer (solid circle) and of the seismic swarms which occurred during 1996 (+) and 1997 (×).

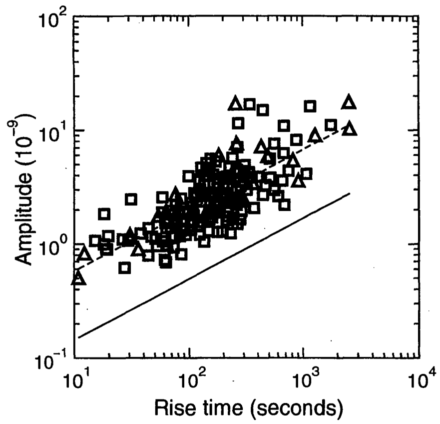

Fig. 4. Amplitude (in nanostrain) versus rise time of the slow earthquakes recorded from 1 February 1996 to 9 September 1997. Negative and positive extensional differences are indicated by triangles and squares, respectively. The dashed line (slope = 0.53 ± 0.04) is the best fit straight line through the experimental points. For each value of the rise time τ, we computed the threshold amplitude is given by the amplitude of the strain signal whose power spectra density (PSD) for a 5τ long window equals the noise PSD (*11*) (solid line).

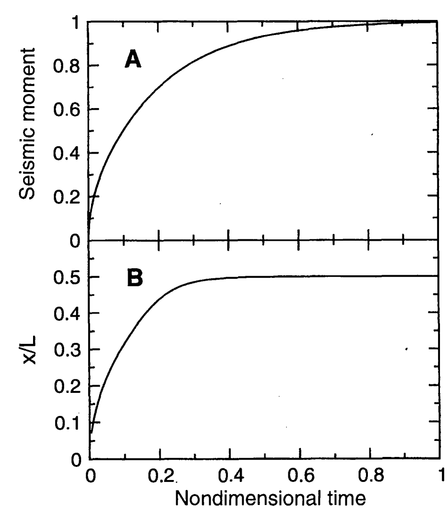

Fig. 5. Time evolution for the 1D fault model described in the text. Initial condition: slip = 0; boundary conditions: slip = 1 at $x = 0$ and slip = 0 at $x = L$. (**A**) Seismic moment; (**B**) position of the point of instantaneous maximum slip rate. Real time is proportional to nondimensional time $\times L^2$.

propagation. We assumed that the inertial term in the dynamic equation is small with respect to the elastic and frictional forces. In the continuous limit, slip as a function of space and time obeys the same diffusion equation as temperature in 1D heat conduction (*22*). The problem of transient conduction in a 1D slab, when the temperature at one side is suddenly changed (slip begins) and the other side is kept at constant zero-temperature (no slip at the fault end), can be analytically resolved (*23*). The time evolution of the seismic moment (proportional to the integral of the slip over the fault) is given by the time evolution of the integral of the temperature and is very similar to the signals recorded by the interferometer (Figs. 1C and 5A). The seismic moment scales with fault width, and rise time scales with width squared. The seismic moment thus scales with the square root of rise time, in agreement with Fig. 4. Although the diffusion equation does not allow us to precisely define the velocity of the slip propagation, the point of maximum instantaneous slip-rate (Fig. 5B) propagates like the rupture in the decreasing velocity model used in (*4*) to fit the only event of the San Andreas sequence related to slow rupture propagation. If the model is realistic, the square root of time scaling would be a property of velocity-strengthening frictional systems in case the seismic moment time history is dominated by slip propagation.

References and Notes

1. I. S. Sacks, S. Suyehiro, A. T. Linde, J. A. Snoke, *Nature* **275**, 599 (1978).
2. M. T. Gladwin, R. L. Gwyther, R. H. G. Hart, K. Breckenridge, *J. Geophys. Res.* **99**, 4559 (1994).
3. I. Kawasaki *et al.*, *J. Phys. Earth* **43**, 105 (1995).
4. A. T. Linde, M. T. Gladwin, M. J. S. Johnston, R. L. Gwyther, R. G. Bilham, *Nature* **383**, 65 (1996).
5. H. Kanamori and E. Hauksson, *Bull. Seismol. Soc. Am.* **82**, 2087 (1992).
6. T. H. Jordan, *Geophys. Res. Lett.* **18**, 2019 (1991).
7. P. F. Ihmlé, P. Harabaglia, T. H. Jordan, *Science* **261**, 177 (1993).
8. P. F. Ihmlé and T. H. Jordan, *Science* **266**, 1547 (1994).
9. J. J. McGuire, P. F. Ihmlé, T. H. Jordan, *Science* **274**, 82 (1996).
10. S. Kedar, S. Watada, T. Tanimoto, *J. Geophys. Res.* **99**, 17893 (1994).
11. The nominal sensitivity of our interferometer is about 3×10^{-12} and its response time is of the order of milliseconds. During the transit of teleseismic waves, it recorded signals as large as 6×10^{-7} and as fast as 10^{-7} s^{-1} without any nonlinearity or abnormal behavior [L. Crescentini, A. Amoruso, G. Fiocco, G. Visconti, *Rev. Sci. Instrum.* **68**, 3206 (1997)].
12. Any interferometer measures the difference in extension between two baselines. From May 1994 to October 1995, we monitored the extension of a 90-m-long baseline (azimuth = N66E) approximately perpendicular to the Apennines, using a 20-cm-long reference baseline (azimuth = N24W). Because laser frequency fluctuations can give spurious signals whose amplitude depends on the difference in length between the two baselines, from December 1995 onward, both baselines were 90 m long and one component of shear strain was measured. Sampling rate was variable until 31 January 1996 and was fixed at 0.5 Hz since then. To avoid ambiguities due to the uneven sampling rate, we discuss data recorded from 1 February 1996 until 9 September 1997, when a power failure stopped data acquisition for a few weeks. However, data recorded before 31 January 1996 do not show any evidence of false signals similar to those discussed above.
13. A. Amoruso, L. Crescentini, R. Scarpa, *Geophys. J. Int.*, in press.
14. K. Kasahara, *Earthquake Mechanics* (Cambridge Univ. Press, Cambridge, 1981), pp. 28–37.
15. The central Apennines are characterized by spatially clustered seismic events; most of these relate to normal faults, oriented parallel with the Apennines (about N35W) and dipping toward the southwest at moderate angles of 40° to 70° [A. Amoruso, L. Crescentini, R. Scarpa, *J. Geophys. Res.* **103**, 29989 (1998); A. Amato *et al.*, *Geophys. Res. Lett.* **25**, 2861 (1998)].
16. Y. Okada, *Bull. Seismol. Soc. Am.* **75**, 1135 (1985).
17. M. Caputo, P. Gasperini, V. Keilis Borok, L. Marcelli, I. Rotwai, *Ann. Geophys.* **130**, 125 (1977); R. Scarpa and A. Zollo, *Earth. Predict. Res.* **1**, 81 (1985); E. Mantovani, D. Albarello, M. Mucciarelli, *Phys. Earth Planet. Inter.* **44**, 264 (1986); G. De Natale, F. Musmeci, A. Zollo, *Geophys. J.* **95**, 285 (1988); W. Marzocchi and F. Mulargia, *Geophys. Res. Lett.* **22**, 29 (1995).
18. D. P. Hill *et al.*, *Science* **260**, 1617 (1993).
19. Seismic moment is proportional to fault slip, length, and width. In the case of small earthquakes, slip and width usually scale with the fault length L (fixed stress-drop and geometric similarity) so that $M_0 \propto L^3 \propto \tau^3$. This last scaling law holds if one assumes that rupture propagates at constant velocity. In the case of large earthquakes, the fault width is independent of the earthquake size, so $M_0 \propto L^2 \propto \tau^2$ or maybe even $M_0 \propto L \propto \tau$ if slip scales with fault width [B. Romanowicz and J. B. Rundle, *Bull. Seismol. Soc. Am.* **83**, 1294 (1993)].
20. There is no general agreement about slow earthquake dynamics. According to some authors, they are not expected from the friction laws as currently formulated [C. H. Scholz, *Nature* **391**, 37 (1998)], while according to others, they are predicted by rate-state laws, under somewhat specialized rheologic properties [C. Marone, *Annu. Rev. Earth Planet. Sci.* **26**, 643 (1998)].
21. I. S. Sacks, A. T. Linde, J. A. Snoke, S. Suyehiro, in *Earthquake Prediction, An International Review*, D. W. Simpson and P. G. Richards, Eds. (Maurice Ewing Series 4, American Geophysical Union, Washington, DC, 1981), pp. 617–628; I. S. Sacks, S. Suyehiro, A. T. Linde, J. A. Snoke, *Tectonophysics* **81**, 311 (1982).
22. Each block of mass m is connected to its two neighbors with springs of stiffness k. Blocks move along the x-direction, and we designate the displacement of a particular block by y_i. Slipping is resisted by the dynamic friction $\beta dy_i/dt$. The motion of a single slipping block is given by

$$m\frac{d^2y_i}{dt^2} = -\beta\frac{dy_i}{dt} + k(y_{i+1} - 2y_i + y_{i-1}) \quad (1)$$

We assume the acceleration (inertial) term to be negligible with respect to the others. The remaining terms are the finite-difference approximation of the ordinary differential equation

$$-\frac{\partial y(x,t)}{\partial t} + \alpha\frac{\partial^2 y(x,t)}{\partial x^2} = 0 \quad (2)$$

Heat diffusion obeys the same equation, which is usually rearranged into nondimensional form by introducing the nondimensional length x/L and the nondimensional time $\alpha t/L^2$. Here, L is the characteristic length of the process.
23. The problem, with different boundary conditions, is discussed in J. H. Lienhard, *A Heat Transfer Textbook* (Prentice-Hall, Englewood Cliffs, NJ, 1981), pp. 152–155.

24. We thank M. R. Carroll, R. L. Gwyther, A. T. Linde, R. Madariaga, J. J. McGuire, and I. S. Sacks for helpful suggestions, and B. Farina for help in screening data. We are also grateful to E. Boschi (president, Istituto Nazionale di Geofisica) for authorizing the use of seismic data and to A. Bettini (director, LNGS) for the logistic support.

26 July 1999; accepted 27 October 1999

Possible Ancient Oceans on Mars: Evidence from Mars Orbiter Laser Altimeter Data

James W. Head III,[1]* Harald Hiesinger,[1] Mikhail A. Ivanov,[1,2] Mikhail A. Kreslavsky,[1,3] Stephen Pratt,[1] Bradley J. Thomson[1]

High-resolution altimetric data define the detailed topography of the northern lowlands of Mars, and a range of data is consistent with the hypothesis that a lowland-encircling geologic contact represents the ancient shoreline of a large standing body of water present in middle Mars history. The contact altitude is close to an equipotential line, the topography is smoother at all scales below the contact than above it, the volume enclosed by this contact is within the range of estimates of available water on Mars, and a series of extensive terraces parallel the contact in many places.

The northern lowlands occupy about one-third of the surface area of Mars (Fig. 1) and have played an important role in its hydrologic and climatic history (*1*). Large outflow channels empty into the northern lowlands (*2*), and a variety of distinctive morphologic features and geologic units occur there (*3–5*). Some investigators have hypothesized that large standing bodies of water, ranging in scale from lakes (*6*) to oceans (*7–10*), may have existed there in past Mars history. High-resolution altimetry data from the Mars Orbiter Laser Altimeter (MOLA) instrument on the Mars Global Surveyor (MGS) mission have underlined the un-

[1]Department of Geological Sciences, Brown University, Providence, RI 02912, USA. [2]Vernadsky Institute, Russian Academy of Sciences, Kosygina 19, 117975, Moscow, Russia. [3]Kharkov Astronomical Observatory, Kharkov University, Sumska 35, 310022, Kharkov, Ukraine.

*To whom correspondence should be addressed.

LINKED CITATIONS

You have printed the following article:

Constraints on Slow Earthquake Dynamics from a Swarm in Central Italy
Luca Crescentini; Antonella Amoruso; Roberto Scarpa
Science, New Series, Vol. 286, No. 5447. (Dec. 10, 1999), pp. 2132-2134.
Stable URL:
http://links.jstor.org/sici?sici=0036-8075%2819991210%293%3A286%3A5447%3C2132%3ACOSEDF%3E2.0.CO%3B2-V

This article references the following linked citations:

References and Notes

[7] **Teleseismic Detection of a Slow Precursor to the Great 1989 Macquarie Ridge Earthquake**
Pierre F. Ihmlé; Paolo Harabaglia; Thomas H. Jordan
Science, New Series, Vol. 261, No. 5118. (Jul. 9, 1993), pp. 177-183.
Stable URL:
http://links.jstor.org/sici?sici=0036-8075%2819930709%293%3A261%3A5118%3C177%3ATDOASP%3E2.0.CO%3B2-2

[8] **Teleseismic Search for Slow Precursors to Large Earthquakes**
Pierre F. Ihmlé; Thomas H. Jordan
Science, New Series, Vol. 266, No. 5190. (Dec. 2, 1994), pp. 1547-1551.
Stable URL:
http://links.jstor.org/sici?sici=0036-8075%2819941202%293%3A266%3A5190%3C1547%3ATSFSPT%3E2.0.CO%3B2-L

[9] **Time-Domain Observations of a Slow Precursor to the 1994 Romanche Transform Earthquake**
Jeffrey J. McGuire; Pierre F. Ihmlé; Thomas H. Jordan
Science, New Series, Vol. 274, No. 5284. (Oct. 4, 1996), pp. 82-85.
Stable URL:
http://links.jstor.org/sici?sici=0036-8075%2819961004%293%3A274%3A5284%3C82%3ATOOASP%3E2.0.CO%3B2-Y

NOTE: *The reference numbering from the original has been maintained in this citation list.*

LINKED CITATIONS

[18] **Seismicity Remotely Triggered by the Magnitude 7.3 Landers, California, Earthquake**

D. P. Hill; P. A. Reasenberg; A. Michael; W. J. Arabaz; G. Beroza; D. Brumbaugh; J. N. Brune; R. Castro; S. Davis; D. dePolo; W. L. Ellsworth; J. Gomberg; S. Harmsen; L. House; S. M. Jackson; M. J. S. Johnston; L. Jones; R. Keller; S. Malone; L. Munguia; S. Nava; J. C. Pechmann; A. Sanford; R. W. Simpson; R. B. Smith; M. Stark; M. Stickney; A. Vidal; S. Walter; V. Wong; J. Zollweg

Science, New Series, Vol. 260, No. 5114. (Jun. 11, 1993), pp. 1617-1623.

Stable URL:

http://links.jstor.org/sici?sici=0036-8075%2819930611%293%3A260%3A5114%3C1617%3ASRTBTM%3E2.0.CO%3B2-D

NOTE: *The reference numbering from the original has been maintained in this citation list.*